Factors determining Poisson's ratio

John J. Zhang and Laurence R. Bentley

ABSTRACT

Poisson's ratio is determined by two independent factors, i.e., the solid rock and dry or wet cracks. The former is influenced by the constituent mineral composition. The higher Poisson's ratio of the rock solid is, the higher is Poisson's ratio of the rock. Poisson's ratio of the solid rock may be roughly estimated from clay contents for clastic rocks. Cracks defined as flat pores of low aspect ratios lower in the dry case or heighten, in the wet case, Poisson's ratio of the rock. The magnitude of change depends on the volume concentration and aspect ratio of cracks. The higher the pore volume concentration and the lower the aspect ratio, the larger is the amount of change in Poisson's ratio. Cracks are also chiefly responsible for the difference between static and dynamic elastic constants and the ratio of static versus dynamic Poisson ratios approaches one when cracks occupy a smaller amount of the total volume.

INTRODUCTION

Poisson's ratio is an important mechanical property and can be used to predict the geomechanical behavior during the drilling of wells and the following recovery processes. Well instability, sand production and hydraulic fracturing are greatly affected by strength parameters, which may relate to its magnitude (Kumar, 1976). Reservoir volume changes due to injection or production and subsequent surface uplift or subsidence can be substantial (Stancliffe and Kooij, 2001). Numerical modelling requires this parameter as input to forecast their influence on wells and surface installations. It is therefore necessary to make reasonable predictions for the purpose of successful oilfield operations.

Conventionally there are two methods to determine this parameter. The first is a uniaxial loading test to compute the ratio of radial strain and axial strain $(\varepsilon_r/\varepsilon_z)$, which is defined as the static Poisson ratio of the rock (ν_s). The second is to measure compressional and shear velocities (V_P and V_S) from seismic data, or sonic well logs, and then to calculate the dynamic Poisson ratio (ν_d) as:

$$\nu_d = \frac{\frac{1}{2}\left(V_P/V_S\right)^2 - 1}{\left(V_P/V_S\right)^2 - 1} \qquad (1)$$

The latter is more advantageous compared to the former in many aspects (Lacy, 1997; Siggins, 1993). For example, velocity measurements are less destructive to the specimen, which may need other testing and measurements, more cost effective and more time efficient. Moreover, the abundance of dynamic Poisson ratio measurements reduces the risk of making incorrect predictions or inferences from given data points. However, dynamic Poisson ratios can be considerably different from static Poisson ratios (Fjaer and Holt, 1994; Fjaer et al., 1992; Gretener, 1994; Siggins, 1993; Tutuncu and Sharma, 1992; Wang, 2000), which is the one used for engineering purposes. There is a necessity to

explore the relationship between static and dynamic measurements before the latter can be widely employed in rock mechanics.

In this paper the authors address two problems encountered in the application of Poisson's ratio. First, the factors that determine the magnitude of a dynamic Poisson ratio will be examined through KT forward modelling (Kuster and Toksoz, 1974). The pore aspect ratio spectra and the elastic moduli of solid rock, which are required in KT forward modelling, are taken from the work by Zhang (2001). The correlation between Poisson's ratio and other elastic moduli is also investigated. Second, the link between dynamic and static Poisson ratios is established from empirical equations or directly from lab measurements reported in the literature. A final goal of this study is to have a comprehensive understanding of Poisson's ratio, and find practical methods of making predictions.

POISSON'S RATIO FROM KT FORWARD MODELLING

The KT theoretical model was derived based on scattering theory. It assumes that pore spaces in rocks can be represented by spheres and oblate spheroids, which are randomly distributed in rock solid. The effective moduli K and μ can be expressed as a function of the elastic moduli of rock solid $(K_s$ and $\mu_s)$ and pore fluid $(K_f$ and $\mu_f)$ and the pore aspect ratio spectrum. The pore aspect ratio spectrum is a series of pore aspect ratios (α_m) and corresponding volume concentrations (c_{α_m}). The pore aspect ratio (α_m) is defined as the ratio of the length of the short axis to that of the long axis on pore cross sections ($\alpha = 1$: spherical pores; $\alpha < 0.1$: cracks or flat pores). The volume concentration c_{α_m} is the volume of pores of aspect ratio α_m divided by the total bulk volume of the rock. The KT equations are as follows (Kuster and Toksoz, 1974):

$$\frac{K - K_s}{3K + 4\mu_s} = \frac{K_f - K_s}{3K_f + 4\mu_s} c_{(\alpha_1)} + \frac{K_f - K_s}{3K_s + 4\mu_s} \sum_{m=2}^{M} c_{(\alpha_m)} \frac{1}{3} T_{iijj(\alpha_m)} \tag{2}$$

$$\frac{\mu - \mu_s}{6\mu(K_s + 2\mu_s) + \mu_s(9K_s + 8\mu_s)} = \frac{\mu_f - \mu_s}{6\mu_f(K_s + 2\mu_s) + \mu_s(9K_s + 8\mu_s)} c_{(\alpha_1)} + \frac{\mu_f - \mu_s}{25\mu_s(3K_s + 4\mu_s)} \sum_{m=2}^{M} c_{(\alpha_m)} [T_{ijij(\alpha_m)} - \frac{1}{3} T_{iijj(\alpha_m)}] \tag{3}$$

where T_{iijj} and T_{ijij} (see Appendix for the relevant formulae) are scalars, dependent on K_s, μ_s, K_f, μ_f, and pore aspect ratio α_m. In order to model the change of effective moduli with effective pressure we have to model the change of the pore aspect ratio spectrum with effective pressure. The expressions to compute the change of the pore aspect ratio spectrum due to an increment in effective pressure can be found in the works by Toksoz et al. (1976) and Zhang (2001).

With the effective moduli (K and μ) calculated in the above equations, the dynamic Poisson ratio (ν_d) is conveniently found by the following formula (Sheriff, 1984):

$$\nu_d = \frac{3K - 2\mu}{2(3K + \mu)} \tag{4}$$

Zhang (2001) inverted velocities at very high effective pressures for the elastic moduli of rock solid for two sets of samples (Han et al., 1986; Khaksar, 2001) by assuming that only spherical pores exist at those pressures. The velocities at very high effective pressures were extrapolated from velocity measurements at a variety of lower effective pressures. With the elastic moduli of rock solid, Zhang (2001) also inverted the velocity measurements for the pore aspect ratio spectra for these samples. In the following we use the elastic moduli of rock solid and the pore aspect ratio spectra to explore the relationship between Poisson's ratio and the factors that may have an effect on it.

POISSON'S RATIO OF THE FRAMEWORK

Poisson's ratio of the framework refers to Poisson's ratio of the rock without fluid saturants (dry rock), and sometimes to Poisson's ratio of the rock with fluid saturants that can flow freely from stressed areas (drained case). As shown in Figure 1 at 30 *MPa*, the data points scatter along the straight line $y = x$, which indicates the effect of Poisson's ratio of rock solid. The strong correlation demonstrates the significance of mineral compositions in the determination of Poisson's ratio at 30 *MPa*. The deviation of data points from the straight line $y = x$ on the lower side suggests that pores decrease Poisson's ratio to varying degrees. Other authors (e.g., Dunn and Ledbetter, 1995; Wang and Nur, 1992) also observed the influence of rock solid and pores on Poisson's ratio. At 100 *MPa* (Figure 2), the data points correlate exceptionally well as they move upward and cluster closer to the straight line $(y = x)$, in which case pores appear to be less instrumental and Poisson's ratio may be used to approximate Poisson's ratio of rock solid. At 10 *MPa* (Figure 3), however, the correlation becomes much worse and pores decrease Poisson's ratio substantially.

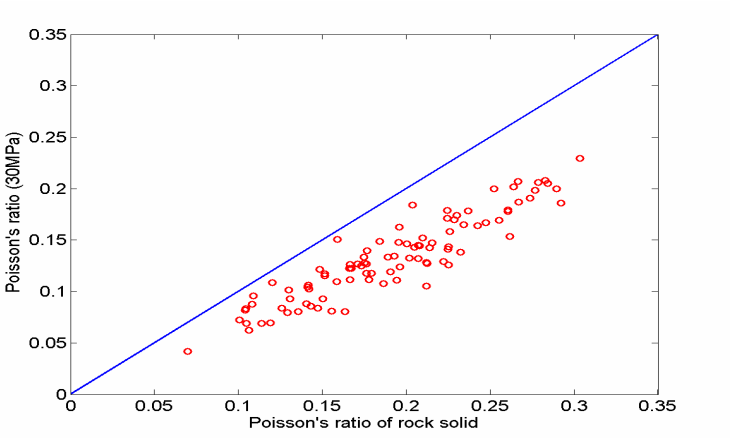

FIG. 1. Poisson's ratio of dry rock versus Poisson's ratio of rock solid at 30 *MPa.*

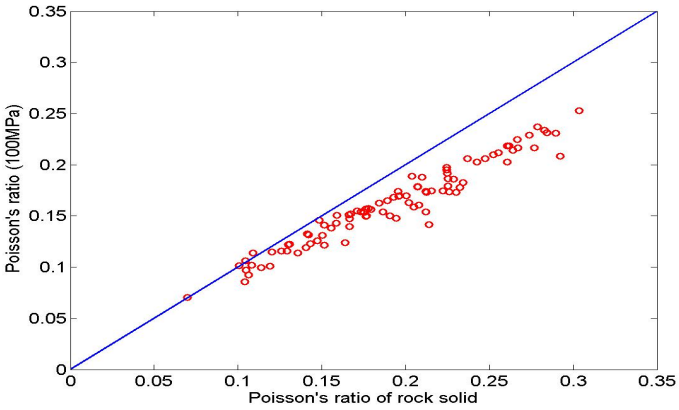

FIG. 2. Poisson's ratio of dry rock versus Poisson' ratio of rock solid at 100 *MPa.*

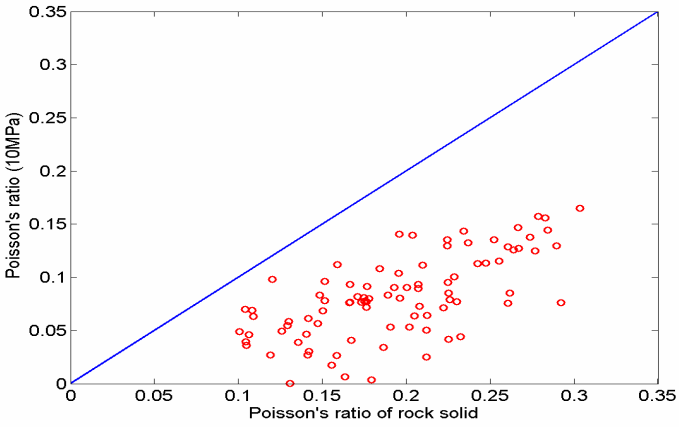

FIG. 3. Poisson's ratio of dry rock versus Poisson' ratio of rock solid at 10 *MPa.*

These three cases show the importance of cracks (pores of low aspect ratios) in Poisson's ratio determination (Berryman, Pride and Wang, 2002; Dunn and Ledbetter, 1995; Walsh, 1965). At low effective pressures, open cracks lower Poisson's ratio so appreciably that Poisson's ratio of rock solid become less important, while at high effective pressures most cracks, especially thin cracks, are closed and Poisson's ratio is primarily influenced by Poisson's ratio of rock solid. Further to demonstrate the effect of cracks, we assumed two cases, rocks with only spherical pores and rocks with only cracks. For the first case, as in Figure 4, Poisson's ratio is nearly equal to Poisson's ratio of rock solid, which appears to demonstrate the insignificance of spherical pores in Poisson's ratio determination.

For the second case, as in Figure 5, the data points at 10 *MPa* scatter in a similar way as in Figure 3, which confirms the insignificance of spherical pores. As mentioned previously, cracks are the dominant factor at this effective pressure.

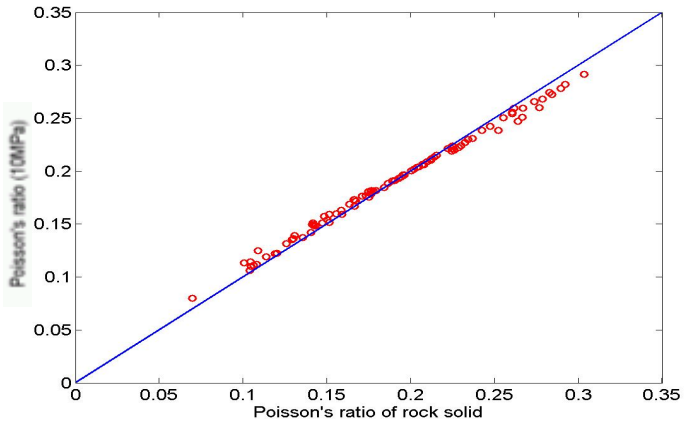

FIG. 4. Poisson's ratio of dry rock (round pores only) versus Poisson' ratio of rock solid.

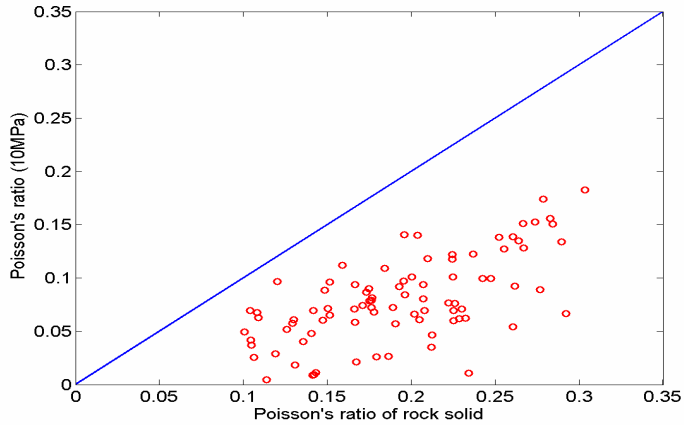

FIG. 5. Poisson's ratio of dry rock (cracks only) versus Poisson' ratio of rock solid.

Cracks can be of different aspect ratios. As shown in Figure 6, thin cracks will decrease Poisson's ratio substantially, while cracks of high aspect ratio, e.g., cracks with aspect ratio equal to 0.1, exert a small influence.

In summary, Poisson's ratio of the framework is determined by two independent factors, cracks and rock solid (mineral compositions). In the presence of considerable amounts of cracks, Poisson's ratio decreases considerably, and the difference in rock solid is marred. The rock solid seems to become less important. With less cracks, especially less thin cracks, the rock solid becomes the primary factor, e.g., at high effective pressures. Spherical pores have little effect regardless of the abundance, which may forecast the insignificance of porosity if it relates to neither of cracks and rock solid.

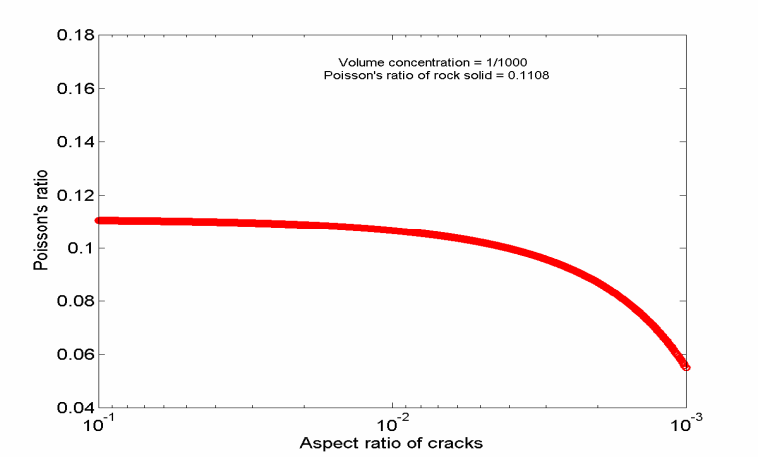

FIG. 6. Poisson's ratio of dry rock versus aspect ratios of cracks.

POISSON'S RATIO OF WET ROCKS

The existence of water in pore space will increase the elastic moduli. The amount of increase fares much higher for the bulk modulus than for the shear modulus, and then Poisson's ratio will increase with water saturation according to equation (1) (Carcione and Cavallini, 2002). As shown in Figure 7, the data points go beyond the straight line $(y = x)$ and demonstrate that, unlike dry pores in Figure 3, water-saturated pores increase Poisson's ratio beyond that of the rock solid. The magnitude of increase, however, is not so drastic as the magnitude of decrease for dry rock, and the data points are closer to the straight line $(y = x)$. The good correlation between Poisson's ratio of wet rocks and Poisson's ratio of rock solid in Figure 7 provides a tool to predict Poisson's ratio of rock solid from Poisson's ratio of wet rocks. Since mineral compositions determine Poisson's ratio of rock solid, Poisson's ratio of wet rocks can be used as an indicator of mineral compositions. This may constitute the rock physics basis for exploration geophysicists, who use Poisson's ratio or V_P/V_S ratio of wet rock to identify lithology (Domenico, 1983; Kithas, 1976; Miller and Stewart, 1990; Pickett, 1963; Rafavich et al., 1984; Wilkens et al., 1984).

To differentiate the effect of spherical pores and cracks, we also calculated two cases, rocks with only spherical pores and rocks with only cracks. For the first case, we predicted a minor effect since water in spherical pores modifies the pore compressibility negligibly, and its influence on shear moduli is almost zero. In Figure 8, the data points sit along the straight line $(y = x)$, which once again confirms the insignificance of spherical pores with respect to mechanical properties. For the second case, the effect should be greater since water in cracks lowers the pore compressibility considerably. As anticipated in Figure 9, Poisson's ratio is elevated considerably as compared with those in Figure 5. The data points are also distributed in similar locations as those in Figure 7, which indicates again the insignificance of spherical pores.

Similarly, the aspect ratio is plotted against Possion's ratio by assuming the same volume concentration and the same rock solid. Figure 10 demonstrates that the lower the aspect ratio, the higher Poisson's ratio. It seems that wet cracks increase Poisson's ratio by the same amount as, or more than, dry cracks decrease Poisson's ratio. By experiments, however, the magnitude of increase is subdued when other cracks exist.

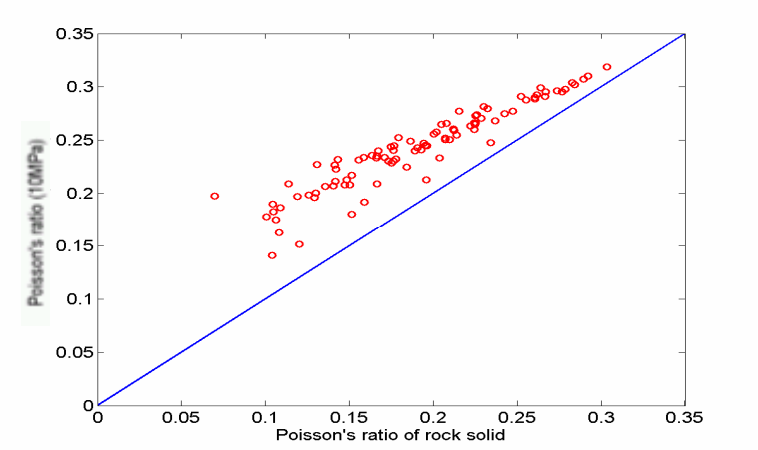

FIG. 7. Poisson's ratio of wet rock versus Poisson' ratio of rock solid at 10 *MPa*.

In conclusion, Poisson's ratio of wet rocks is determined by both wet cracks and rock solid. The former increases Poisson's ratio, but the magnitude of increase is not drastic, so that the data points do not deviate from Poisson's ratio of rock solid, and a good correlation between Poisson's ratio of wet rocks and Poisson's ratio of rock solid is maintained

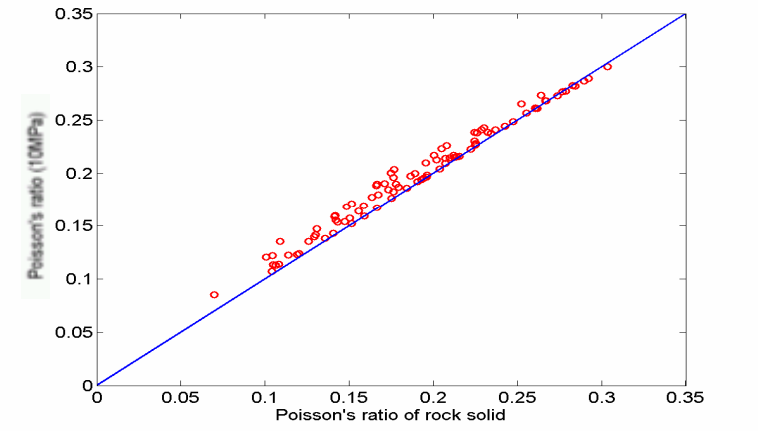

FIG. 8. Poisson's ratio of wet rock (round pores only) versus Poisson' ratio of rock solid.

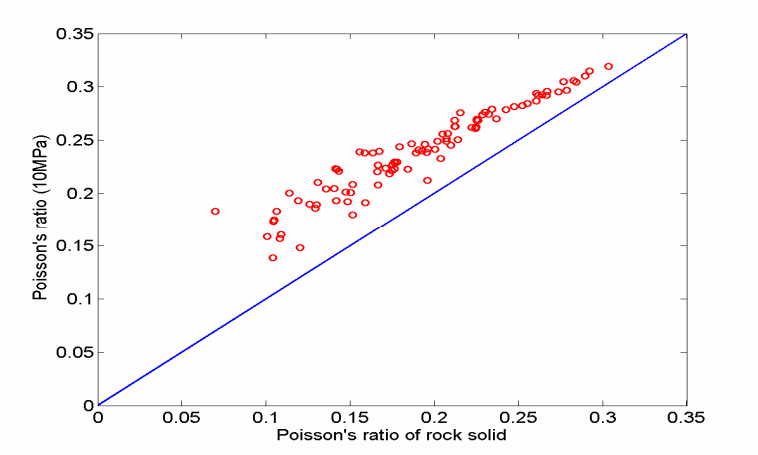

FIG. 9. Poisson's ratio of wet rock (cracks only) versus Poisson' ratio of rock solid.

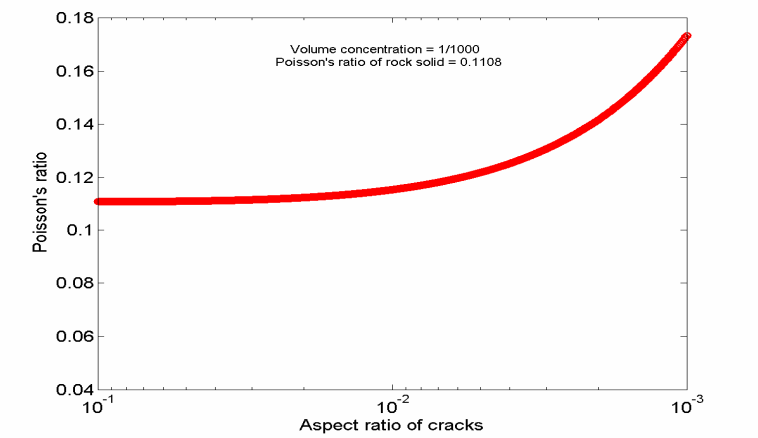

FIG. 10. Poisson's ratio of wet rock versus aspect ratios of cracks.

RELATION OF POISSON'S RATIO TO THE ELASTIC MODULI

Strength parameters (compressive strength and tensile strength), which are essential to forecast sand production, well instability, and hydraulic fracturing, are observed to be linked to the magnitude of elastic moduli (after Fjar et al., 1992). The higher the elastic moduli, the larger the strength parameters. If Poisson's ratio is correlated with the elastic moduli, then it can be used to estimate strength parameters to some degree. In the following section, we will discuss how they relate to each other.

Unlike Poisson's ratio, the bulk, shear and Young moduli are also affected by round pores. Theoretically speaking, Poisson's ratio won't correlate to the elastic moduli due to the presence of spherical pores. When cracks play a dominant role, however, they are

related since they all depend on cracks. In order to avoid further complication, we assumed the same rock solid and computed the elastic moduli and Poisson's ratio (in the dry case) at an effective pressure of 10 *MPa*. As shown in Figure 11, a correlation is exhibited between Poisson's ratio and Young's modulus of the framework (dry rock). The higher Poisson's ratio, the larger is Young's modulus, which is reasonable since higher Poisson ratios imply less cracks, which implies a higher Young modulus. The scatter of data points is chiefly due to the effect of round pores on Young's modulus. At high pressures, the amount of cracks becomes small, and Young's modulus is affected by both round pores and rock solid while Poisson's ratio is mostly determined by rock solid. Under these conditions, they are not correlated. Poisson's ratio at 10 *MPa* is also directly related to the bulk modulus (Figure 12) and the shear modulus.

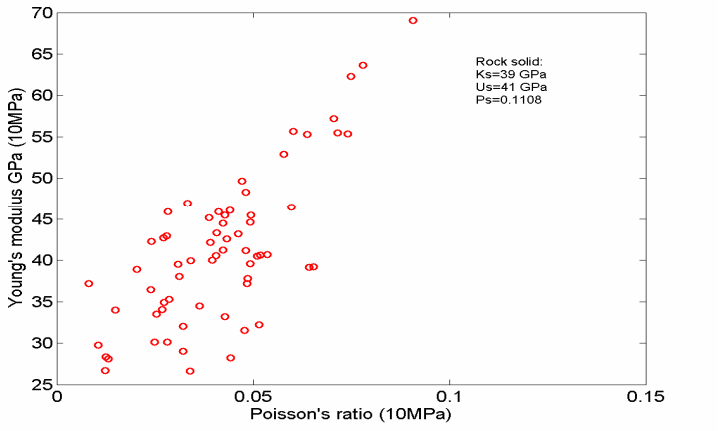

FIG. 11. Poisson's ratio versus Young's modulus of dry rock at 10 *MPa.*

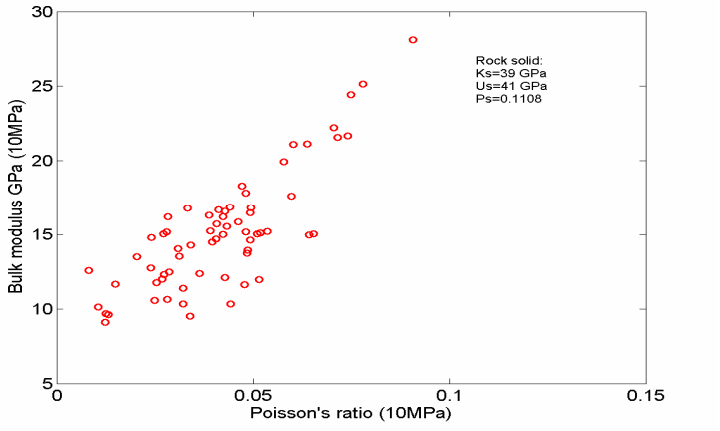

FIG. 12. Poisson's ratio versus bulk modulus of dry rock at 10 *MPa.*

When rocks are water saturated, the relationship is reverse since wet cracks increase Poisson's ratio. In Figure 13, Poisson's ratio varies inversely with Young's modulus. The higher Poisson's ratio, the lower is Young's modulus.

When the rock solid changes as it does in many real cases, it adds another complication to their relationship. Even at low effective pressures, the correlation for dry rocks may be so weak that Poisson's ratio cannot be used to predict the elastic moduli as in Figure 14. For water-saturated rocks, the correlation is better (Figure 15).

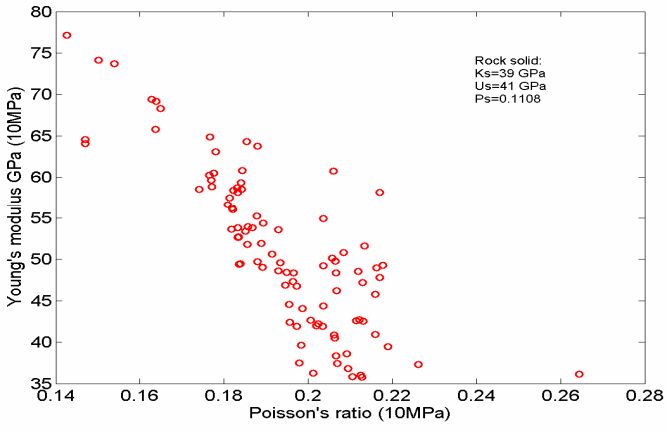

FIG. 13. Poisson's ratio versus Young's modulus of wet rock at 10 *MPa*.

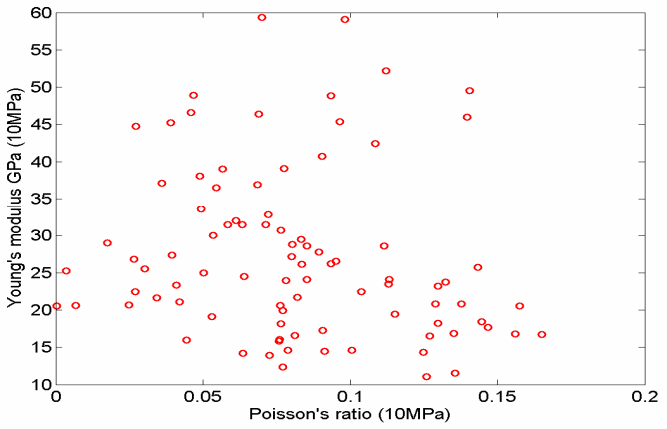

FIG. 14. Poisson's ratio versus Young's modulus of dry rock at 10 *MPa.*

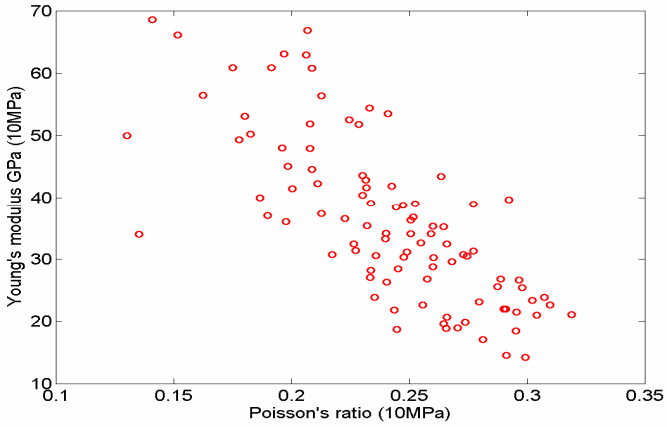

FIG. 15. Poisson's ratio versus Young's modulus of wet rock at 10 *MPa.*

STATIC POISSON RATIO VERSUS DYNAMIC POISSON RATIO

Poisson's ratio discussed in the previous sections is the dynamic one, which differs from the static one used for geomechanical applications. The discrepancy between these two results from strain amplitude and frequency. Sonic logs and wave laboratory tests send signals through the sample at small stress and strain. Static tests apply large stress, which generate large strain. The former is elastic while the latter has a considerable portion of irrecoverable deformation. This leads to static versus dynamic Young's, bulk and shear moduli of less than one. Winkler (1979) showed that sonic velocities in sandstones decreased as strain amplitude measurements increased. The magnitude of static versus dynamic Poisson ratios depends on how static versus dynamic moduli change, and by experiments the ratio is mostly greater than one. The irrecoverable deformation derives from the existence of cracks. When strain amplitude is large enough, it collapses cracks and the strain is not recoverable. For non-porous and crack-free materials such as steel, static versus dynamic Poisson ratios are close to one (Wang, 2001).

At high frequencies as in dynamic tests, pore fluids do not have enough time to equilibrate the pressure distribution, and the rock appears to be stiffer. At low frequencies as in static tests, pore fluids have enough time to reach pressure equilibrium among pore spaces, and the rock behaves less stiffly. This results in velocity dispersion, another reason why static/dynamic moduli are less than one. The velocity dispersion arises due to the existence of cracks.

Consequently, cracks play a central role in static versus dynamic elastic moduli and Poisson's ratio (Bristow, 1960). A rough estimate of the abundance of cracks is the magnitude of elastic moduli, and how high effective pressure is. When elastic moduli are large or effective pressures are high, cracks are rendered less as the ratio of static versus dynamic Poisson ratios approaches one (Cheng and Johnston, 1981; Simmons and Brace, 1968; Wang, 2001). As shown in Figure 16, static versus dynamic Poisson ratios measured for siltstone tend toward one with increasing Young moduli (Yale and

Jamieson, Jr., 1994). The regression line may be used to predict the ratio from Young's modulus. Unfortunately we have not collected a complete set of data to demonstrate the relation of static versus dynamic Poisson ratios to effective pressure. However, the trend is direct and obvious. With increasing effective pressure, the static versus dynamic Poisson ratio will gradually decrease to one.

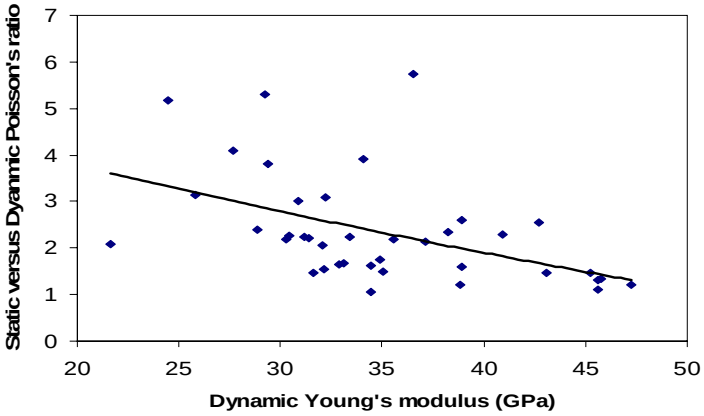

FIG. 16. Static/Dynamic Poisson's ratio versus Dynamic Young's modulus of dry rock.

DISCUSSION AND CONCLUSIONS

Poisson's ratio is determined by cracks and rock solid. Dry cracks decrease Poisson's ratio while wet cracks increase Poisson's ratio at a slower pace. The magnitude of decrease or increase depends on the amount of cracks and crack aspect ratio. The larger a volume percentage and the lower an aspect ratio the cracks have, the more decreases or increases Poisson's ratio. Round pores have little effect on Poisson's ratio. The relationship between Poisson's ratio and other physical properties lies in the relationship between cracks and these physical properties. For example, porosity is in direct proportion to cracks in a gas field of west Australia, and Poisson's ratio (wet rocks) was then found to vary directly with porosity in Figure 17. Another example is compaction and erosion. Compaction leads to loss of both porosity and crack concentrations while erosion rebound recovers them partly. Accordingly, Poisson's ratio (wet rocks) will decrease with compaction and increase with erosion. Accurate calculation needs a description of porosity and cracks under compaction or erosion.

The rock solid can be significant in the case of less cracks, e.g., at high effective pressure. Poisson's ratio of rock solid depends on mineral compositions. For our samples of clastic rocks, it depends chiefly on clay content. Figure 18 shows the increase of Poisson's ratio with the increase of clay content, which provides a practical way to make rough estimates of Poisson's ratio of rock solid from clay content.

Poisson's ratio can be correlated with the elastic moduli if cracks are dominant. For dry rocks, Poisson's ratio varies directly with Young, bulk and shear moduli. For wet rocks, Poissons's ratio tends to increase with decreasing Young, bulk and shear moduli. The quantitative relationships may provide a simple rule to guess the elastic moduli and then strength parameters from Poisson's ratio.

To find practical application in geomechanics, a dynamic Poisson ratio should convert to a static Poisson ratio. It may be feasible to use relationships such as that shown in Figure 16 to calculate the ratio of static over dynamic Poisson ratio.

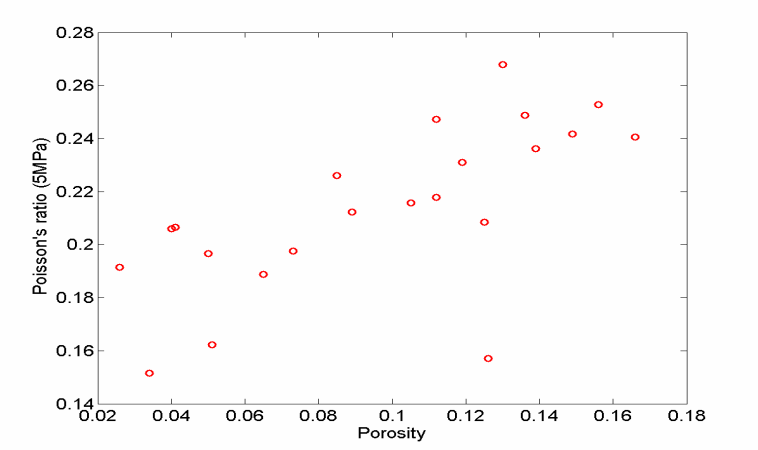

FIG. 17. Porosity versus Poisson's ratio (wet rock) in a gas field of west Australia.

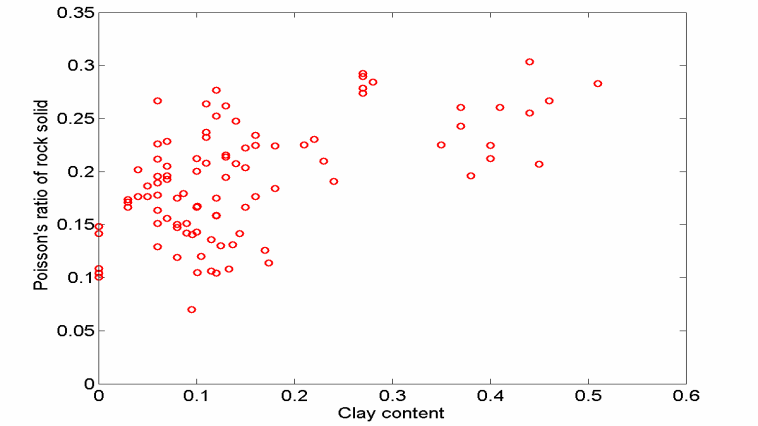

FIG. 18. Clay content versus Poisson's ratio of rock solid.

ACKNOWLEDGEMENTS

We would like to express our appreciation to Rakhit Petroleum Consulting Ltd. and the CREWES project for the support of this research. We also gratefully acknowledge discussions with and suggestions from Stephen Burnie, Dean Provins and Xiang Wang .

REFERENCES

Berryman, J. G., S. R. Pride and H. F. Wang, 2002, A differential scheme for elastic properties of rocks with dry or saturated cracks, Geophys. J. Int., **151**, 597-611.

Bristow, J. R., 1960, Microcracks, and the static and dynamic elastic constants of annealed and heavily cold-worked metals, British Journal of Applied Physics, **11**, 81-85.

Carcione, J. M. and F. Cavallini, 2002, Poisson's ratio at high pore pressure, Geophysical Prospecting, **50**, 97-106.

Cheng, C. H. and D. H. Johnston, 1981, Dynamic and static moduli, Geophysical Research Letter, **8**, 39-42.

Domenico, S. N., 1984, Rock lithology and porosity determination from shear and compressional wave velocity, Geophysics, 1188-1195.

Dunn, M. L. and H. Ledbetter, 1995, Poisson's ratio of porous and microcracked solids: theory and application to oxide superconductors, Journal of Materials Research, **10**, 2715-2722.

Fjaer E. and Rune, M. Holt, 1994, Rock acoustics and rock mechanics: Their link in petroleum engineering, The Leading Edge, **13**, 255-258.

Fjaer E., R. M. Holt, P. Horsrud, A. M. Raaen and R. Risnes, 1992, Petroleum related rock mechanics: Elsevier Science Publishers B. V.

Gretener, Peter E., 1994, Reflections on the Keck visiting professorship at the Colorado School of Mines and the interdisciplinary dialog, The Leading Edge, **13**, 1022-1026.

Han, De-hua, A. Nur and Dale Morgan, 1986, Effects of porosity and clay content on wave velocities in sandstones, Geophysics, **51**, 2093-2107.

Khaksar, A., C. M. Griffiths and C. McCann, 1999, Compressional- and shear-wave velocities as a function of confining stress in dry sandstones, Geophysical Prospecting, **47**, 487-508.

Kithas, B. A., 1976, Lithology, gas detection and rock properties from acoustic logging system, SPWLA 17th Ann. Logging Symp., R1-R10.

Kumar, J, 1976, The effect of Poisson's ratio on rock properties: The 51st Annual Fall Technical Conference and Exhibition of the Society of Petroleum Engineering of AIME, SPE 6094.

Kuster, Guy T. and M. Nafi Toksoz, 1974, Velocity and attenuation of seismic waves in two-phase media: part 1. Theoretical formulations, Geophysics, **39**, 587-606.

Lacy, Lewis L., 1997, Dynamic rock mechanics testing for optimized fracture designs: The 1997 SPE Annual Technical Conference and Exhibition, SPE 38716.

Miller, S. L. M. and R. R. Stewart, 1990, Effects of lithology, porosity and shaliness on P- and S-wave velocities from sonic logs, Can. J. Expl. Geoph., **26**, 94-103.

Pickett, G. R., 1963, Acoustic character logs and their application in formation evaluation, JPT, 659-667.

Rafavich, F., Kendall, C. H. St. C., and T. P. Todd, 1984, The relationship between acoustic properties and the petrographic character of carbonate rocks, Geophysics, **49**, 1622-1636.

Sheriff, Robert E., 1984, Encyclopedic dictionary of exploration geophysics, SEGSiggins, Anthony F., 1993, Dynamic elastic tests for rock engineering, in Comprehensive Rock Engineering: Principles, Practice and Projects, volume **3**, Eds by John A. Hudson, 601-618.

Simmons, G. and W. F. Brace, Comparison of static and dynamic measurements of compressibility of rocks, JGR, **70**, 5649-5656.

Stancliffe, R. P. W. (Stan) and Marco W. A. van der Kooij, 2001, The use of satellite-based radar interferometry to monitor production activity at the Cold Lake heavy oil field, Alberta, Canada, AAPG, **85**, 781-793.

Toksoz, M. N., C. H. Cheng and A. Timur, 1976, Velocities of seismic waves in porous rocks, Geophysics, **41**, 621-645.

Tutuncu, A. N. and M. M., Sharma, 1992, Relating static and ultrasonic laboratory measurements to acoustic log measurements in tight gas sands: The 67th SPE Annual Technical Conference and Exhibition, SPE 24689.

Walsh, J. B., 1965, The effect of cracks in rocks on Poisson's ratio, Journal of Geophysical Research, **70**, 5429-5257.

Wang, Z., 2001, Dynamic versus static elastic properties of reservoir rocks, in Seismic and Acoustic Velocities in Reservoir Rocks, volume 3, Eds by Zhijing Wang and Amos Nur, 531-539.

Wang, Z. and A. Nur, 1992, Elastic wave velocities in porous media: A theoretical recipe, in Seismic and Acoustic Velocities in Reservoir Rocks, volume 2, Eds by Zhijing Wang and Amos Nur, 1-35.

Wilkens, R., Simmons, G. and L. Caruso, 1984, The ratio V_p/V_s as a discriminant of composition for siliceous limestones, Geophysics, **18**, 50-1860.

Winkler, K., 1979, Effects of pore fluids and frictional sliding on seismic attenuation, Ph.D. Thesis, Stanford University.

Yale, D. P. and W. H. Jamieson, Jr., 1994, Static and dynamic mechanical properties of carbonates, in Rock Mechanics: A. A. Balkema, Rotterdam.

Zhang, J. J., 2001, Time-lapse seismic surveys: Rock physics basis, M.Sc. Thesis, University of Calgary.

Settari, Antonin and F. M. Mourits, 1998, A coupled reservoir and geomechanical simulation system, SPE Journal, 219-226.

Walters, D. A. and A. Settari, 2000, Poreelastic effects of cyclic steam stimulation in the Cold Lake Reservoir, SPE 62590.

Wang, Zhijing and A. Nur, 2000, Seismic and acoustic velocities in reservoir rocks, recent developments, Geophysics reprint series.

APPENDIX A

$$T_{iijj} = \frac{3F_1}{F_2}$$
$$T_{ijij} - \frac{1}{3}T_{iijj} = \frac{2}{F_3} + \frac{1}{F_4} + \frac{F_4F_5 + F_6F_7 - F_8F_9}{F_2F_4} \qquad \text{(A.1)}$$

where

F1=1-[3/2(g+θ)-R(3/2g+5/2θ-4/3)]

F2=1-[1+3/2(g+θ)-R/2(3g+5θ)]+B(3-4R)-1/2(3B-1)(3-4R)(g+θ-R(g-θ+2θ^2)

F3=1-1/2(R(2-θ)+(1+α^2)/α^2g(R-1))

F4=1-1/4[3θ+g-R(g-θ)]

F5=Bθ(3-4R)-R(g+θ-4/3)+g

F6=B(1-θ)(3-4R)-g+R(g+θ) (A.2)

F7=2-1/4[9θ+3g-R(5θ+3g)]+Bθ(3-4R)

F8=B(1-θ)(3-4R)-1+2R-g/2(R-1)-θ/2(5R-3)

F9=Bθ(3-4R)-g(R-1)+Rθ

B=1/3 K_f/K_s

R=$3\mu_s/(3K_s+4\mu_s)$

θ=α/[(1-α^2)^(3/2)](αcos(α)-α(1-α^2)^0.5)

g=α^2/(1-α^2)(3θ-2)